

Article

$^{87}\text{Sr}/^{86}\text{Sr}$ Ratios and Atmospheric Noble Gases in Theistareykir Geothermal Fluids: A Record of Glacial Water

Daniele Luigi Pinti ^{1,*} , Marie Haut-Labourdette ², André Poirier ¹, Marion Saby ¹, Vincent J. van Hinsberg ³, Kim Berlo ³, Maria Clara Castro ⁴, Bjarni Gautason ⁵ and Ásgerður K. Sigurðardóttir ⁶

¹ Geotop & Département des Sciences de la Terre et de l'Atmosphère, Université du Québec à Montréal, Montreal, QC H3C 3P8, Canada; poirier.andre@uqam.ca (A.P.); saby.marion@courrier.uqam.ca (M.S.)

² Department of Geology and Geoenvironment, National & Kapodistrian University of Athens, Panepistimiopolis, 10679 Athens, Greece; mariehl99@yahoo.fr

³ Geotop & Department of Earth and Planetary Sciences, McGill University, Montreal, QC H3A 0G4, Canada; vincent.vanhinsberg@mcgill.ca (V.J.v.H.); kim.berlo@mcgill.ca (K.B.)

⁴ Department of Earth and Environmental Sciences, University of Michigan, Ann Arbor, MI 48109-1005, USA; mccastro@umich.edu

⁵ ISOR Iceland GeoSurvey, Urðarhvarf 8, 203 Kopavogur, Iceland; bjarni.gautason@isor.is

⁶ Landsvirkjun, Háaleitisbraut 68, 103 Reykjavík, Iceland; asgerdur.sigurdardottir@landsvirkjun.is

* Correspondence: pinti.daniele@uqam.ca; Tel.: +1-514-987-3000 (ext. 2572)



Citation: Pinti, D.L.;

Haut-Labourdette, M.; Poirier, A.; Saby, M.; van Hinsberg, V.J.; Berlo, K.; Castro, M.C.; Gautason, B.; Sigurðardóttir, Á.K. $^{87}\text{Sr}/^{86}\text{Sr}$ Ratios and Atmospheric Noble Gases in Theistareykir Geothermal Fluids: A Record of Glacial Water. *Geosciences* **2022**, *12*, 119. <https://doi.org/10.3390/geosciences12030119>

Academic Editors:

Giovanni Vespasiano,
Massimiliano Vardè,
Carmine Apollaro and
Jesus Martinez-Frias

Received: 8 February 2022

Accepted: 1 March 2022

Published: 4 March 2022

Publisher's Note: MDPI stays neutral with regard to jurisdictional claims in published maps and institutional affiliations.



Copyright: © 2022 by the authors. Licensee MDPI, Basel, Switzerland. This article is an open access article distributed under the terms and conditions of the Creative Commons Attribution (CC BY) license (<https://creativecommons.org/licenses/by/4.0/>).

Abstract: The determination of the current and past recharge sources, as well as the reconstruction of the timing of the recharge in geothermal reservoirs, is required in order to correctly assess the resource potential of these systems. Theistareykir is a newly developed geothermal field close to the well-known exploited fields of Krafla and Námafjall in NE Iceland. In this study, the $^{87}\text{Sr}/^{86}\text{Sr}$ ratios measured in deep geothermal fluids are presented and, together with the Cl and noble gas signatures, are used to place constraints on the fluid sources. The Cl/Sr and $^{87}\text{Sr}/^{86}\text{Sr}$ ratios show a peculiar and unique composition among Icelandic geothermal fluids. The $^{87}\text{Sr}/^{86}\text{Sr}$ ratios range from 0.70355 to 0.70671, suggesting the presence of a significant seawater component—possibly marine aerosols added to rain or snowfall—as well as an additional source of Sr leached from local basalts. Moreover, a correlation between the atmospheric noble gas (ANGs) elemental ratios Ne/Ar, Kr/Ar and Xe/Ar, and the $^{87}\text{Sr}/^{86}\text{Sr}$ ratios is observed. The latter results from the mixing of meteoric water with Sr leached from local basalts, meteoric water containing unrelated Sr from seawater, and recharge water with ANGs derived from trapped air bubbles in snow. We suggest that the combined ANGs and Sr seawater signatures are representative of a glacial water source derived from the melting of compacting snow.

Keywords: $^{87}\text{Sr}/^{86}\text{Sr}$; atmospheric noble gases; geothermal fluids; seawater; glacial water; Theistareykir; Iceland

1. Introduction

The radiogenic Sr isotope ratio ($^{87}\text{Sr}/^{86}\text{Sr}$) is a robust tracer of surface water, groundwater and geothermal fluid sources [1–7]. Studies on the isotopic signature of the radiogenic Sr in hot and mineral springs [2] and geothermal wells [1,3,7] have evidenced a direct relationship between the $^{87}\text{Sr}/^{86}\text{Sr}$ ratios in the spring waters and the surrounding rocks, indicating that the main source of dissolved strontium is the leaching of Sr-bearing minerals such as plagioclase, feldspar or micas contained in volcanic, metamorphic or sedimentary country rocks. The relationships between $^{87}\text{Sr}/^{86}\text{Sr}$ ratios and elemental ratios such as Ca/Sr or Cl/Sr in fluids were helpful to identify the presence of at least three sources of Sr in geothermal fluids: local bedrock [2,3,7]; seawater, especially in coastal areas' geothermal fields (e.g., Taupo, New Zealand [7] and Reykjanes, Iceland [1]); and a hydrothermal source with $^{87}\text{Sr}/^{86}\text{Sr}$ ratios similar to those observed in local bedrock, but displaying high Ca/Sr

and Cl/Sr ratios, possibly indicating hydrothermal calcite precipitation, which is a sink for dissolved Sr [7].

Noble gases—He, Ne, Ar, Kr and Xe—are also excellent tracers of geothermal fluid sources. They are inert, and have distinct isotopic signatures among the terrestrial reservoirs: the mantle, the crust, and the atmosphere [8–13]. Meteoric waters, which are generally assumed to be the most abundant fluid in a magmatic–hydrothermal system [14], contain atmospherically derived noble gases (or ANGs hereafter). The ANGs enter the reservoir at the recharge, where they are dissolved at the solubility equilibrium of the water table (the Air Saturated Water component, or ASW [15]). The isotopic signatures are those of the atmosphere, but their elemental ratios (e.g., Ne/Ar, Kr/Ar, Xe/Ar) are those expected for the ASW, although Byrne et al. [16] have recently suggested that ANGs could be fractionated by boiling processes taking place in the reservoir. Magmatic fluids acquire mantle-derived noble gases such as helium, which shows an enrichment in solar ^3He over ^4He , with a $^3\text{He}/^4\text{He}$ or “R/Ra” (where Ra = 1.384×10^{-6} is the atmospheric ratio) ratio value of 8 ± 1 for the depleted mantle [17], and 45–60 for the primitive mantle [18]. It should also be common for hydrothermal fluids to contain Ne, Ar and Xe mantle-derived isotopes [19], but they are often diluted by the meteoric-ASW component beyond recognition [20]. Finally, crustal fluids are dominated by the radiogenic ^4He and $^{40}\text{Ar}^*$ (* stands for the radiogenic fraction of Ar) produced in the reservoir rocks by U, Th and K decay [21].

Strontium and noble gas isotopes (mainly He) have traditionally been measured and analyzed together in magmatic rocks [22] but rarely in associated geothermal fluids, as Sr and He are often decoupled by secondary processes such as boiling, which affects volatiles but not the dissolved Sr [23] or different transport mechanisms and sources [2]. As an example, Notsu et al. [2] observed a decoupling between the measured $^3\text{He}/^4\text{He}$ ratios and $^{87}\text{Sr}/^{86}\text{Sr}$ in the mineral springs of Japan because the former is mainly transported from mantle melts to the surface by degassing through faults, whereas Sr is extracted from local rocks. Sr–He systematics in geothermal fluids have been primarily analyzed to determine the contributions of subducting sediments in volcanic-arc settings [20,24,25], and—in some successful cases—to identify magmatic heat sources [26].

Here, the $^{87}\text{Sr}/^{86}\text{Sr}$ composition measured in geothermal fluids collected from production wells of the high-enthalpy geothermal field of Theistareykir, in northeastern Iceland is presented. This is a newly operating geothermal field for which the noble gas geochemistry was studied in detail by Saby et al. [27]. To our knowledge, however, Sr isotopes were previously unavailable in these fluids. Our goal is to take advantage of the observed correlations between Sr isotopes and ANGs in order to investigate the presence of past and modern glacial water, and to reconstruct the glacial recharge history of this geothermal reservoir. This is a departure from the traditional use of the ANGs as a tracer of multi-phase partitioning processes such as boiling or injectate invasion in geothermal reservoirs [8,16,26,28].

2. Geological Background

Theistareykir is a high-enthalpy liquid-dominated field located at the intersection of the Northern Volcanic Zone (NVZ, Figure 1a)—corresponding to the northeastern branch of the Mid-Atlantic oceanic ridge—and the WNW–ESE-oriented transform zone known as the Tjörnes Fracture Zone [29,30]. It is ~30 km NW of the Krafla and Námafjall geothermal fields, the latter being the oldest producing geothermal fields in Iceland. The exploitation of the Theistareykir field began in 2017, with a total of 18 wells, with depths varying between 1723 m and 2799 m. The plant currently has two generating units of 45 MWe, and is the fourth largest geothermal power station in Iceland in terms of power produced.

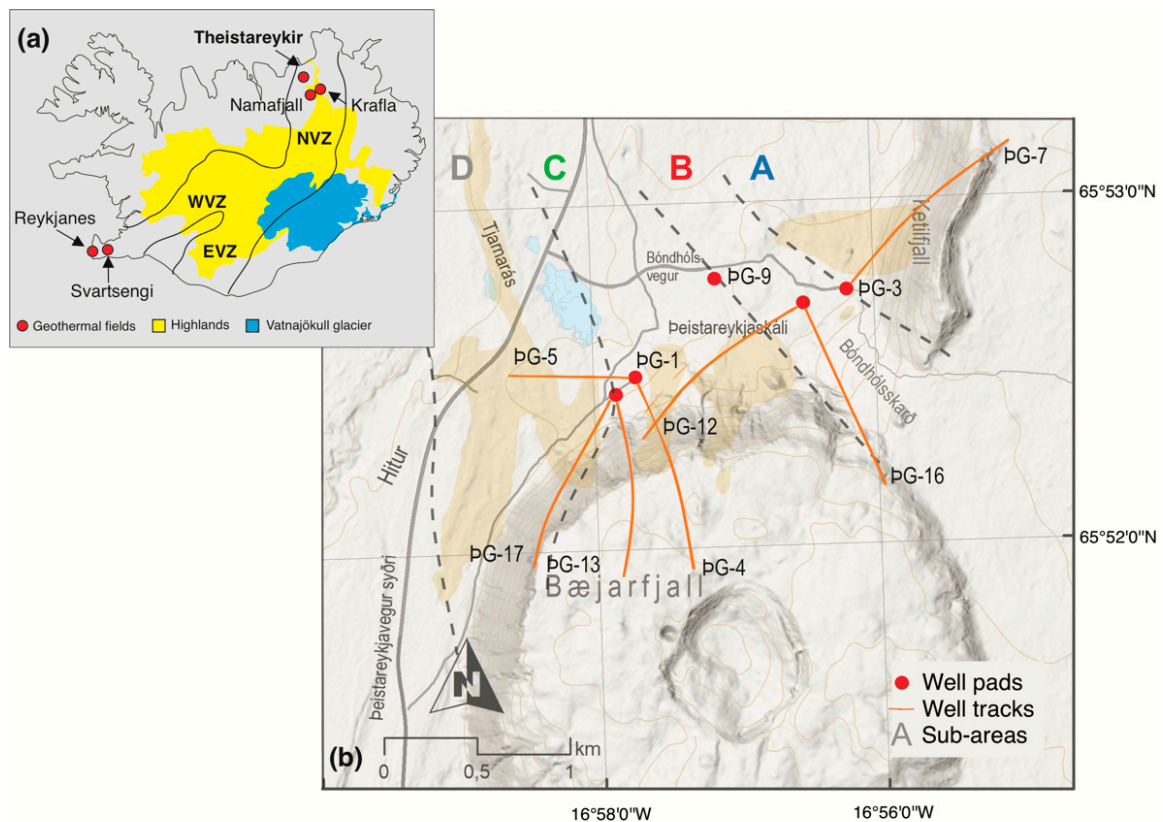


Figure 1. (a) Iceland, with the locations of the main geothermal sites cited in the text, and the location of the Iceland Highlands with major glaciers. Abbreviations: NVZ = Northern Volcanic Zone; WVZ: Western Volcanic Zone; EVZ = Eastern Volcanic Zone. (b) Detailed map of the production area of the Theistareykir geothermal field, with the sampled wells and the subareas defined by [31].

Theistareykir is a volcanic fissure system that includes the Theistareykjarbunga shield volcano. The volcanic products are mainly tholeiitic basalt lava flows. These include the Skildingahraun (>14.5 ka) lava shield; Stóravíti, a widespread (30 km³) post-glacial lava shield that erupted approximately 10.5 ka ago [32]; the picritic Borgarhraun (10–8 ka); and the youngest Theistareykjahraun lava shield (2.4 ka) [33]. The bedrock is composed of basalt hyaloclastite ridges formed by subglacial eruptions during the Ice Age, interglacial lava flows, and the recent lava flows mentioned above. Olivine-tholeiites with MgO contents higher than 7–8 wt% and picrites (MgO > 9–13 wt%) are the main lithologies, with a few silicic rocks of andesitic and rhyolitic composition found on the western side of the field.

The reservoir is cross-cut by dykes and sills filling fractures and fissures that mainly strike N-S and NNE-SSW but also WNW-ESE and E-W [30]. These intrusive bodies, together with fractures and alteration zones, are the main permeability areas of the reservoir [29], and act as aquifers [34]. A broadband 2-D MT survey indicated that the hydrothermal reservoir consists of two parts: one shallower, down to 1000-m depths and water-dominated with average temperatures of 205 °C, and one deeper, down to 5000 m and boiling, with temperatures of 300–350 °C or higher [34].

The average porosity of the reservoir is ~10%, while the average permeability (k) is $1 \times 10^{-15} \text{ m}^2$ (ca. 1 md [35]). Variable degrees of alteration from shallower clays and zeolites (50–200 °C) to deeper epidote (>250 °C) are observed in the reservoir [36]. The heat is possibly sourced by an E-W trending intrusive magmatic source [37] located at minimal depths of 4000–8000 m [34]. A detailed petrographic study on the picritic Borgarhaun lava flow at Theistareykir suggests that these magmatic products were transported from near-Moho depths to the surface in days, with little to no interaction with the crust [38].

The Theistareykir geothermal area covers 30 km², but the production zone is restricted to an 11 km² area around the 533 m-high Mt. Bæjarfjall, which would be the nearest area of meteoric water recharge in the field (Figure 1b). The chemical, isotopic and temperature differences measured in the surface manifestations (fumaroles, mudpots) during the initial exploration phases lead to the subdivision of the Theistareykir field into five zones, from east to west: A = Mount Ketilfjall; B = Bóndhólsskarð; C = Theistareykjagundur; D = Tjarnarás, and E = the Western Margin [29,31] (Figure 1b).

The geochemistry of the fluids produced is dominated by Na-K-Cl with a TDS value of about 350 mg/L and a pH range of 7.8–9.1. The dry gas phase accompanying the fluids is dominated by CO₂ (45–81%), followed by H₂S (7–78%), N₂ (1–8%), H₂ (0.2–3.8%) and CH₄ (0.01–0.03%) [39].

The water-stable isotopes ($\delta^2\text{H}$ and $\delta^{18}\text{O}$) and noble gases were analyzed in the Theistareykir production well fluids by Saby et al. [27]. These fluids display some of the lowest recorded $\delta^2\text{H}$ and $\delta^{18}\text{O}$ values in Iceland's geothermal fluids [40]. This depletion is thought to be the result of glacial water recharge, possibly from the Holocene age, in the geothermal reservoirs of the NVZ (Theistareykir, Krafla and Námafjall) [41]. Saby et al. [27] identified at least four sources of fluids based on noble gases and water-stable isotopes: (1) local modern meteoric water, (2) sub-modern meteoric water from the southern highlands, (3) pre-Holocene glaciated meteoric water with calculated U-Th/He and K-Ar fluid residence times from 57 ± 20 ka to 160 ± 80 ka, and (4) a ³He-enriched magmatic fluid. Saby et al. [27] highlighted the ubiquitous presence of atmospheric and ASW components in both the deep fluids and surface manifestations, but the origin of these atmospheric components was not investigated.

3. Materials and Methods

Ten production wells (PG-1, 3, 4, 5, 6, 7, 12, 13, 16, 17) were sampled at Theistareykir in the summer of 2017, shortly after production began. All of the samples were analyzed for their Sr isotopic composition, as well as their noble gas concentrations and isotopic composition. The chemical composition of these fluids is determined yearly during summer surveys by the National Power Company of Iceland, Landsvirkjun, and the data reported in this study refers to the summer 2017 survey. The water samples were obtained at the wellhead using a portable field water/steam separator. The water samples were filtered (0.45 μm) during collection, acidified with nitric acid (Suprapur, Sigma-Aldrich, Darmstadt, Germany), and analyzed for Sr concentrations by ICP-MS at the ALS laboratories, Luleå, Sweden. The water samples for the determination of the Cl concentration were filtered (0.45 μm) during collection, and were analyzed by Ion Chromatograph (IC) at the geochemical laboratory that the Landsvirkjun company owns at the Krafla geothermal field. The sampling details and analysis procedures can be found in [42].

The fluid samples were collected at the wellhead in pre-cleaned Nalgene 250 mL bottles without chemical treatment using a portable fluid/steam separator for the Sr isotopic measurements. The bottles were rinsed three times with well fluids prior to collection. Fluid was removed through evaporation until a residual salt containing at least 20 ng total Sr was left. Classic Sr-resin (Eichrom, Lisle, IL, USA) ion chromatography (double-pass) was used to ensure the purification of the Sr from potential Rb isobaric interference. All of the reagents were double distilled within class 100 enclosures in DST-1000 sub-boiling stills (Savillex, Eden Prairie, MN, USA), and were diluted with Milli-Q ultrapure water (MilliporeSigma, Burlington, MA, USA). Measurement by multi-collector plasma mass spectrometer (Nu Plasma II, Nu Instruments, Wrexham, UK) with an Aridus II desolvating membrane (Teledyne CETAC technologies, Omaha, NE, USA) was carried out at the Radiogenic and Non-traditional Stable Isotopes laboratory of Geotop, Montreal. "On-peak-zero" gas blank measurements were carried out in order to account for imperfect small residual washout and krypton interferences (coming from the plasma's argon gas supply; Praxair, QC, Canada). The mass bias was corrected by normalizing to $^{86}\text{Sr}/^{88}\text{Sr} = 0.1194$. The NBS987 Sr standard was measured during the analytical sessions, and yielded an $^{87}\text{Sr}/^{86}\text{Sr}$ ratio of 0.71024 ± 0.00002 .

Noble gases were sampled from the gas phase separated at the wellhead using a portable fluid/steam separator. The gas was collected in a 14 cm³ standard refrigeration-grade type K 3/8" copper tube. The copper tube was directly installed at the gas exit of the portable fluid/steam separator using all stainless-steel Swagelok[®] NPT connections. After letting the gas flow for several minutes, the tubes were sealed using stainless steel pinch-off clamps, and were closed using an electric drill to minimize air contamination [27].

Except for samples PG-7 and PG-17, all of the other samples were analyzed for noble gases at the Noble Gas Laboratory of the University of Michigan. Samples PG-7 and PG-17 were analyzed at the Noble Gas laboratory (GRAM) of Geotop, Montreal. At the University of Michigan, gas samples connected to a stainless-steel purification line were dried on a molecular sieve trap, and their reactive gases were removed using three Ti-getters at 600 °C for three minutes each. The noble gases were quantitatively extracted using a computer-controlled cryo-separator at temperatures of 49 K (He), 84 K (Ne), 225 K (Ar), 280 K (Kr), and 320 K (Xe) respectively, and sequentially were allowed to enter a Thermo[®] Helix SFT mass spectrometer for He and Ne isotope analyses, and a Thermo[®] ARGUS VI mass spectrometer for Ar, Kr, and Xe isotope analyses. The typical blanks were 0.04 to 0.15% of the measured sample value, respectively. The quantitative analyses were obtained by calibrating the two mass spectrometers with a known aliquot of standard air. The calculated standard errors for concentrations ranged from 1.3 to 2.2% of the measured values. See [21] for further details.

At Geotop, the gases from the copper tubes were collected in a pre-evacuated 12cc stainless-steel finger equipped with a bellow valve. The finger was connected to a stainless-steel extraction line, and the reactive gases were removed onto two Ti-getters at 600 °C for 15 min each, and a SAES ST-707 getter at 100 °C for 15 min. The gases were then adsorbed onto an ARS[®] cryogenic trap containing activated charcoal, and released sequentially at 40 K, 110 K, 210 K, and 280 K for He, Ne, Ar, and Kr-Xe, respectively. The noble gas isotopes were measured on a Thermo[®] HELIX-MC Plus. Blanks were routinely measured, and were typically on the order of 0.01% for ⁴He to 0.15% for ¹³²Xe. The quantitative analyses were obtained by calibration with a known aliquot of standard air. The calculated standard errors for the concentrations ranged from 1 to 3% of the measured values. See [43] for further details.

4. Results

Table 1 reports the Sr and Cl concentrations in ppm in the volume (mg/L) measured in the residual fluid phase sampled at the wellhead by the Landsvirkjun company, together with the ⁸⁷Sr/⁸⁶Sr measured at Geotop, as well as the F-value fractionation factors for the atmospheric noble gas ratios ²⁰Ne/³⁶Ar, ⁸⁴Kr/³⁶Ar and ¹³²Xe/³⁶Ar, normalized against their atmospheric ratio, as follows:

$$F(i) = [i/^{36}\text{Ar}]/[i/^{36}\text{Ar}]_{\text{air}} \quad (1)$$

The resulting values are defined as the F-values for each "i" noble gas isotope of atmospheric origin. These F-values are fractionation factors that provide a measure of enrichment or depletion of noble gases relative to the atmospheric air composition (e.g., [44]).

The Sr and Cl concentrations and ⁸⁷Sr/⁸⁶Sr ratios are original (this study), and the noble gas F-values are from Saby et al. [27], except for sample PG-7, which was reanalyzed due to the abnormally low ³⁶Ar concentrations.

The chlorine and Sr contents in the residual water range from 52 to 105 ppm, and from 0.001 to 0.005 ppm, respectively (Table 1). The ⁸⁷Sr/⁸⁶Sr ratios range from 0.70355 ± 0.00004 in sample PG-5 to 0.70671 ± 0.00008 in sample PG-6. Finally, F(²⁰Ne), F(⁸⁴Kr) and F(¹³²Xe) range from 0.451 to 0.667, from 1.458 to 2.293, and from 2.473 to 3.508, respectively (Table 1).

Table 1. Cl, Sr, $^{87}\text{Sr}/^{86}\text{Sr}$ and ANG F-values for Theistareykir geothermal fluids and fluid endmembers.

Well	Cl (ppm)	Sr (ppm)	$^{87}\text{Sr}/^{86}\text{Sr}$	\pm	F(^{20}Ne)	\pm	F(^{84}Kr)	\pm	F(^{132}Xe)	\pm
ÞG-1	96.26	0.005	0.70376	0.00003	0.520	0.020	1.721	0.068	3.240	0.166
ÞG-3	80.2	0.005	0.70358	0.00003	0.546	0.020	1.719	0.068	3.097	0.158
ÞG-4	59.71	0.002	0.70466	0.00015	0.480	0.018	1.667	0.066	3.176	0.162
ÞG-5	61.08	0.002	0.70355	0.00004	0.451	0.016	1.659	0.066	3.508	0.180
ÞG-6	173.03	0.004	0.70671	0.00008	0.521	0.020	1.789	0.072	3.337	0.170
ÞG-7	18.52	0.005	0.70564	0.00004	0.667	0.012	1.458	0.029	2.473	0.063
ÞG-12	86.88	0.002	0.70602	0.00004	0.509	0.018	1.590	0.064	3.169	0.162
ÞG-13	70.94	0.002	0.70452	0.00009	0.596	0.011	1.678	0.033	3.068	0.078
ÞG-16	52.53	0.001	0.70650	0.00007	0.533	0.010	1.658	0.033	2.926	0.075
ÞG-17	85.09	0.001	0.70467	0.00007	0.587	0.018	2.293	0.068	3.171	0.102
Seawater ¹	18980	13	0.709225	0.00005	0.298	-	1.865	-	3.381	-
Basalt ²	45	141.42	0.70320	0.00005	-	-	-	-	-	-
Air	-	-	-	-	1	-	1	-	1	-
ASW ³	-	-	-	-	0.249	-	2.027	-	4.009	-

¹ $^{87}\text{Sr}/^{86}\text{Sr}$ ratio from [45]. ² Cl and Sr from [46]; $^{87}\text{Sr}/^{86}\text{Sr}$ ratio from [1]; F-values calculated following [47] at 15 °C and a salinity of 35 g/L. ³ F-values calculated following [48] at 3.7 °C and a salinity of 0 g/L.

5. Discussion

5.1. Strontium Origin in the Theistareykir Fluids

The measured $^{87}\text{Sr}/^{86}\text{Sr}$ ratios in the Theistareykir fluids range from 0.70355 to 0.70671 (Table 1). The lowest value is slightly higher than those measured in the Holocene tholeiitic basalts of Theistareykir (0.702847–0.703215 [49], Table S1), while the highest value has rarely been observed in the geothermal fluids of Iceland [1]. The $^{87}\text{Sr}/^{86}\text{Sr}$ ratios measured in deep geothermal fluids vary from 0.70327 to 0.70457, with high values being found primarily in the geothermal fields of the Reykjavik peninsula (e.g., Reykjanes, Svartengi; Figure 1a and [1]). The geothermal fluids sampled at Krafla and Námafjall, the two geothermal fields closest to Theistareykir, have $^{87}\text{Sr}/^{86}\text{Sr} = 0.7040 \pm 0.0003$ [1].

There are two notable exceptions: Kasthvatnslaug ($^{87}\text{Sr}/^{86}\text{Sr} = 0.7058$ [1]), a cold spring (24 °C) 18 km SW of the Theistareykir field, and a cold spring named Helgavatn ($^{87}\text{Sr}/^{86}\text{Sr} = 0.70654 \pm 0.00006$ [1]), in Northwest Iceland, significantly far away from the region of interest. These springs were sampled in the 1970s, and their data were included in internal reports of the Iceland National Energy Authority (Orkustofnun). The origin of the radiogenic $^{87}\text{Sr}/^{86}\text{Sr}$ ratios, however, was not provided.

The probabilistic density distribution histograms of 812 values of $^{87}\text{Sr}/^{86}\text{Sr}$ measured in Iceland fluids, mineral and rocks (Table S1, Supplementary Material for the compiled data) suggest that the sole plausible source of high- $^{87}\text{Sr}/^{86}\text{Sr}$ Theistareykir fluids is seawater (Figure 2). However, even in Reykjanes, where the geothermal fluid is 100% seawater, the $^{87}\text{Sr}/^{86}\text{Sr}$ ratio is 0.7040, closer to that of local basalt rather than that of seawater (0.709225). This is the result of water–rock interactions at very high temperatures, which produce the alteration minerals epidote and chlorite, which are important sinks for Sr [50]. Consequently, epidote would have high $^{87}\text{Sr}/^{86}\text{Sr}$ ratios, as measured in Reykjanes (up to 0.7073 [51]), while the residual geothermal fluid would be depleted in radiogenic ^{87}Sr , and would reach a close equilibrium with the local hosting basaltic rocks [1]. The exceptions are the hydrothermal fluids of the submarine sediment-hosted Grimsey hydrothermal field, located in the Tjörnes Fracture Zone, with $^{87}\text{Sr}/^{86}\text{Sr}$ ratios very close to those of the local seawater (0.709225). Here, seawater penetrates the shallow levels of the basaltic seafloor at low temperatures, and mixes with a 250 °C hydrothermal effluent to be rapidly discharged from the smokers, without reaching equilibrium with the hosted sediments [45].

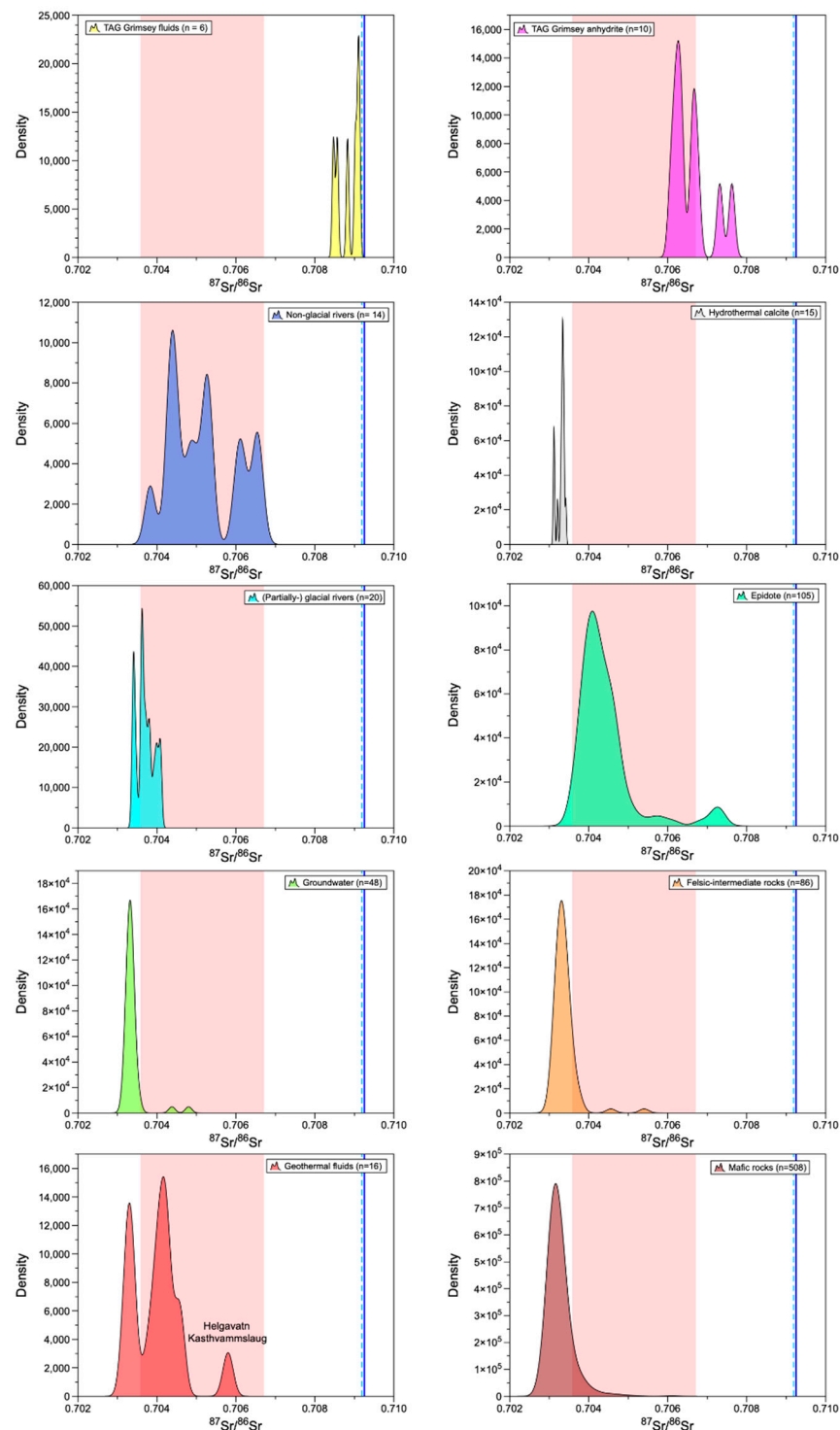


Figure 2. Probabilistic density histograms of the $^{87}\text{Sr}/^{86}\text{Sr}$ ratios in the fluids, minerals and rocks of Iceland. The red band indicates the range of $^{87}\text{Sr}/^{86}\text{Sr}$ values measured in the Theistareykir fluids. The blue line is the seawater value [45], while the dashed blue line is for glacier ice [52]. See Table S1 for the values. The bibliographic references for the geothermal fluids are [1,52]; groundwater are [53,54]; non-glacial, partially- and glacial rivers are [52,53]; TAG Grimsey fluids and anhydrite is [45]; hydrothermal calcite is [53]; epidote are [51,55]; and mafic, intermediate, and felsic igneous rocks are [49,51,56–73].

In Theistareykir, epidote also occurs such that any seawater infiltrating the reservoir and exchanging Sr with epidote should have reached nearly equilibrium with the local

basaltic rocks with respect to $^{87}\text{Sr}/^{86}\text{Sr}$. However, this is not observed and Theistareykir fluids show rather high $^{87}\text{Sr}/^{86}\text{Sr}$ values up to 0.70672 (Table 1). Because the exchange of Sr between the fluid and the epidote depends on the temperature and the duration of the exchange, at Theistareykir we should assume that the seawater-derived Sr was introduced recently or at low temperatures.

Seawater infiltration into geothermal reservoirs is not suggested for high-temperature geothermal fields in Northeastern Iceland, and the Cl-contents of the fluids are low. The chemistry of the geothermal fluids at Theistareykir is Na-K-Cl, but the Cl contents in the reservoir are thought to be related to the condensation of acidic magmatic vapor [31].

Figure 3 shows the $^{87}\text{Sr}/^{86}\text{Sr}$ ratios versus the Cl/Sr mass ratios for all of the Icelandic geothermal fluids [1,7,74], including those measured at Theistareykir (this study). Icelandic geothermal fluids other than Theistareykir are either a mixture between water which has interacted with local basalt (Cl/Sr = 0.318, [46,75]; $^{87}\text{Sr}/^{86}\text{Sr} \leq 0.7032$ [58]) and seawater (Cl/Sr = 2559 and $^{87}\text{Sr}/^{86}\text{Sr} = 0.709225$); or a mixture of water that has interacted with local basalt (labeled “WRI” for water-rock interaction in Figure 3) and an endmember characterized by a very high Cl/Sr $\approx 1.1 \times 10^5$ (from data extrapolation) and $^{87}\text{Sr}/^{86}\text{Sr} = 0.70337$ [53]. This endmember (here labelled “magmatic fluid”) is present in other geothermal systems, such as Taupo (New Zealand), and is interpreted as representing a pristine deep geothermal fluid, which is affected by seawater to a lesser extent [7]. In Theistareykir, the high Cl/Sr ratio of this geothermal endmember can be the result of two concomitant processes: the enrichment of Cl through magma degassing [76], and the depletion of Sr trapped in hydrothermal calcite during high-temperature reactions in the reservoir (e.g., [7]).

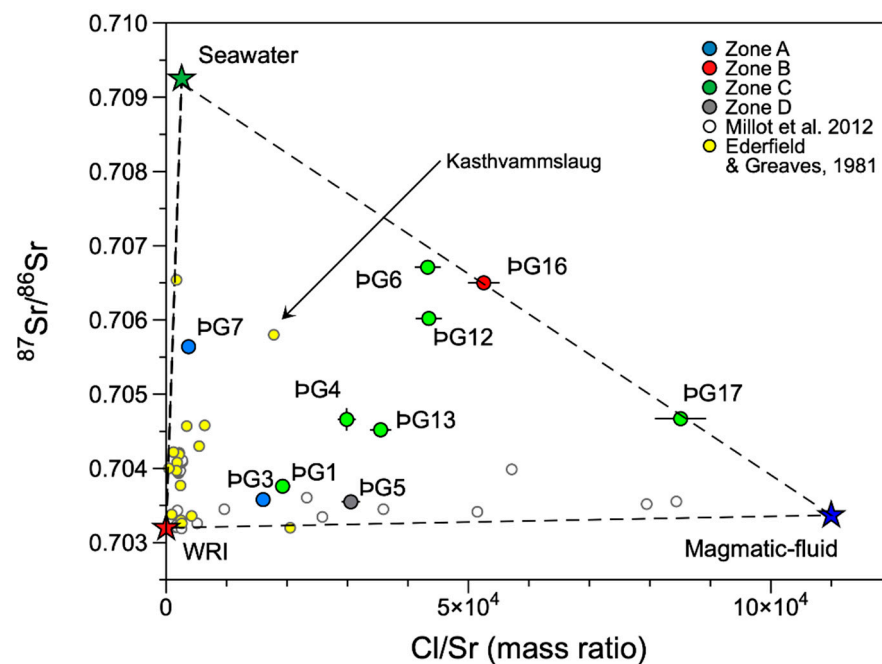


Figure 3. The Cl/Sr mass ratio vs. the $^{87}\text{Sr}/^{86}\text{Sr}$ ratio of Theistareykir hydrothermal fluids (the color represents the subzones of the field, see Section 2 for details), compared to the literature data from other geothermal fields of Iceland. See the text for details on the endmember compositions. The white dots are data from Figure 5 of [7], redrawn (data unpublished).

The Sr content of Theistareykir fluids shows a pattern which is different from that of other fields (Figure 3), resulting from a mixture of all three sources (Figure 3). Their respective contributions can be estimated from data reported in Table 1 using equations from [77]:

$$^{87}\text{Sr}/^{86}\text{Sr}_{\text{sample}} = ^{87}\text{Sr}/^{86}\text{Sr}_{\text{hydrothermal}} \times H + ^{87}\text{Sr}/^{86}\text{Sr}_{\text{basalt}} \times B + ^{87}\text{Sr}/^{86}\text{Sr}_{\text{seawater}} \times S \quad (2)$$

$$(\text{Cl}/\text{Sr})_{\text{sample}} = H \times (\text{Cl}/\text{Sr})_{\text{hydrothermal}} + B \times (\text{Cl}/\text{Sr})_{\text{basalt}} + S \times (\text{Cl}/\text{Sr})_{\text{seawater}} \quad (3)$$

$$H + B + S = 1 \quad (4)$$

where H, B and S are the fraction of Sr in the magmatic, seawater and basalt endmember in the mixture. The relative proportions of each source to Sr in the Theistareykir well fluids are reported in Table 2.

Table 2. Proportions (in %) of each source of Sr in the Theistareykir fluids.

Well	Magmatic-Fluid (%)	Seawater (%)	WRI (%)
ÞG-1	17.30	8.77	73.93
ÞG-3	14.44	5.88	79.68
ÞG-4	26.60	23.38	50.02
ÞG-5	27.65	5.01	67.34
ÞG-6	38.00	56.95	5.05
ÞG-7	2.43	40.26	57.31
ÞG-12	38.43	45.53	16.04
ÞG-13	31.76	20.93	47.31
ÞG-16	46.77	<0.01	53.23
ÞG-17	76.84	22.14	1.02
Krafla ¹	2.08	2.75	95.17
Námafjall ¹	0.69	16.84	82.47
Reykjanes ¹	1.57	16.65	81.78

¹ Estimated from Sr and Cl data reported by [1], for comparison.

It is worth noting that these mixing proportions are related to the Sr content of the fluid, not the mass of the fluid itself. In other words, e.g., sample ÞG-6 contains nearly 57% Sr derived from seawater, but 57% of the fluid is not seawater (which would give a Cl content of 10,818 ppm, nearly 60 times that of the measured value; Table 1).

There is, in the mixture, a fourth fluid devoid of both Cl and Sr, which is local meteoric water (which, in northeastern Iceland, seems not to contain seawater aerosols), leading to the dilution of the Cl and Sr concentrations while leaving the elemental or isotopic ratios unchanged. Icelandic rainwater is impacted by seawater salt spray, as is evidenced by the identical element ratios and a systematic decrease in the concentrations and element ratios with distance from the ocean (e.g., [78]). It is estimated that typical Icelandic rainwater contains 1‰ seawater [79], which would give a Cl content of ~19 ppm and 0.007 ppm Sr. In contrast, pristine rainwater away from the oceans is estimated to contain only 0.18 ppm, and essentially no Sr [80]. The Cl and Sr of a pure atmospheric meteoric component is thus negligible compared to the seawater input.

Compared to the neighboring Krafla and Námafjall fields, Theistareykir has a major contribution of Sr from the magmatic and seawater sources. The Theistareykir seawater component is higher than the seawater-dominated Reykjanes field (Table 2). Interestingly, among the samples of [1], the closest in terms of chemistry (Cl/Sr ratio) and Sr isotopic composition to the Theistareykir fluids is Kásthvammslaug, 18 km to the SW, possibly suggesting similar sources of Sr and mixing ratios to those of the Theistareykir reservoir fluids.

Figure 4 shows the water-stable isotopic ratio $\delta^{18}\text{O}$ vs. the $^{87}\text{Sr}/^{86}\text{Sr}$ ratio, which suggests that Theistareykir fluids might represent a mixture of several sources enriched in radiogenic ^{87}Sr .

In Figure 4, a hypothetical mixing line is drawn (blue dashed line) between seawater ($\delta^{18}\text{O} = 0\text{‰}$ by definition and $^{87}\text{Sr}/^{86}\text{Sr} = 0.709225$ [45]) and a meteoric recharge component from the southern Highlands of Iceland ($\delta^{18}\text{O} = -13.2\text{‰}$ [27]), which has likely acquired Sr from the leaching of local tholeiitic basalts ($^{87}\text{Sr}/^{86}\text{Sr} \leq 0.7032$ [49,58]). Except for ÞG6, ÞG12 and ÞG16, all of the samples plot on a mixing trend (within the 95% confidence interval, i.e., the light-grey dashed lines of Figure 4) of a seawater-highlands water mixture. However, it is worth noting that sample ÞG-16, which Figure 3 would suggest is a mixture of seawater and the magmatic endmember, here points to an $^{87}\text{Sr}/^{86}\text{Sr}$ ratio intermediate

between that of fluid–rock interaction and seawater. On the other hand, the $\delta^{18}\text{O}$ of -13.58‰ measured in PG-16 does not indicate an interaction with seawater. The latter is very similar or just slightly depleted compared to the expected value for the Highlands recharge ($\delta^{18}\text{O} = -13.2\text{‰}$). Sample PG-16 could therefore represent a meteoric water component entering the geothermal reservoir, with its $\delta^{18}\text{O}$ signature being progressively shifted (see the arrow in Figure 4) towards values of -8‰ , or possibly higher, by water–rock interactions with tholeiitic basalts ($\delta^{18}\text{O} = -6.5\text{‰}$ [27]). This modified water component could subsequently mix with meteoric Highlands water, creating the trend represented by the dashed orange straight line of Figure 4.

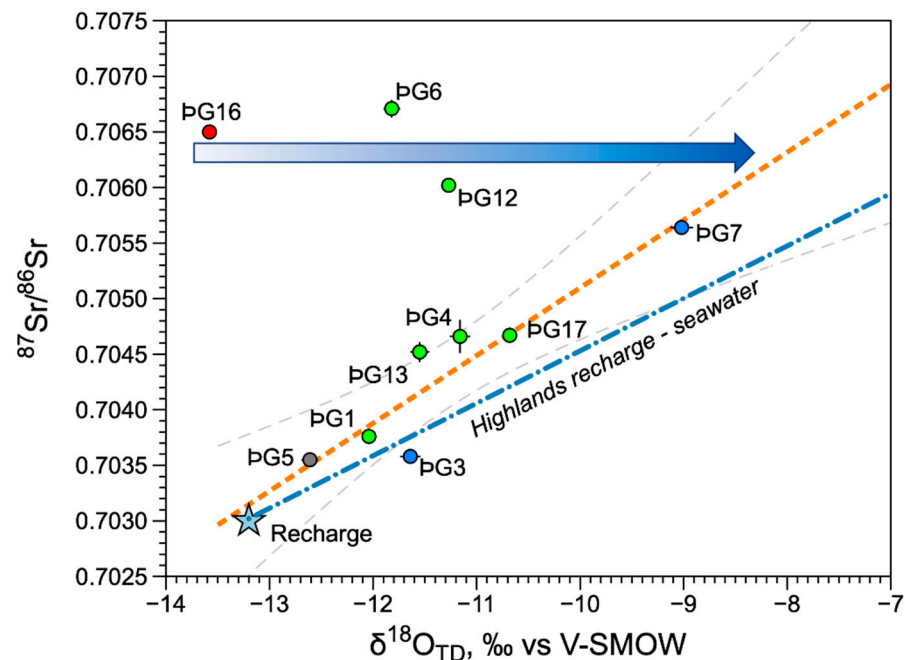


Figure 4. Water-stable isotope ratio $^{18}\text{O}/^{16}\text{O}$ (in delta notation vs. V-SMOW) vs. the $^{87}\text{Sr}/^{86}\text{Sr}$ ratio of Theistareykir hydrothermal fluids. The colors of the symbols are the same as those in Figure 3. See the text for further details.

The question arises of which water source may have a “seawater” Sr content while displaying the stable isotopic composition characteristic of meteoric water. In Iceland, non-glaciated rivers show relatively high $^{87}\text{Sr}/^{86}\text{Sr}$ ratios of up to 0.70659 (Table S1). This is because seawater aerosols are transported and introduced into the Iceland river network through rainfall or snowfall [52]. For example, Hindshaw et al. [52] measured the $^{87}\text{Sr}/^{86}\text{Sr}$ in ice samples from the southern glacier Langjökull, and obtained a value of 0.70919, which is very similar to that of the local seawater value (0.709225). If sample PG-16 is representative of glacial water, either modern or of Holocene-Quaternary age from the southern Highlands [27,81], it may contain a dominant seawater Sr source. The stable isotopes, however, would reflect those of the main water mass, i.e., glacial water. The Sr and H_2O would be decoupled due to mass-balance constraints. Because seawater is significantly higher in Sr, the sole addition of a small seawater component will impact both the Sr content and the isotopic signature disproportionately.

Newly observed correlations between atmospheric noble gases and Sr isotopes may provide additional independent evidence of this glacial water recharge in the Theistareykir field. This is discussed below.

5.2. Correlations between ANGs and Sr in Theistareykir Geothermal Fluids

The calculated atmospheric noble gas ratios $^{20}\text{Ne}/^{36}\text{Ar}$, $^{84}\text{Kr}/^{36}\text{Ar}$ and $^{132}\text{Xe}/^{36}\text{Ar}$ are higher than those expected for equilibrium solubility at recharge conditions (a Mean Annual Air Temperature (MAAT) of 3.7 °C [27]), using solubility data from [48] (Figure 5).

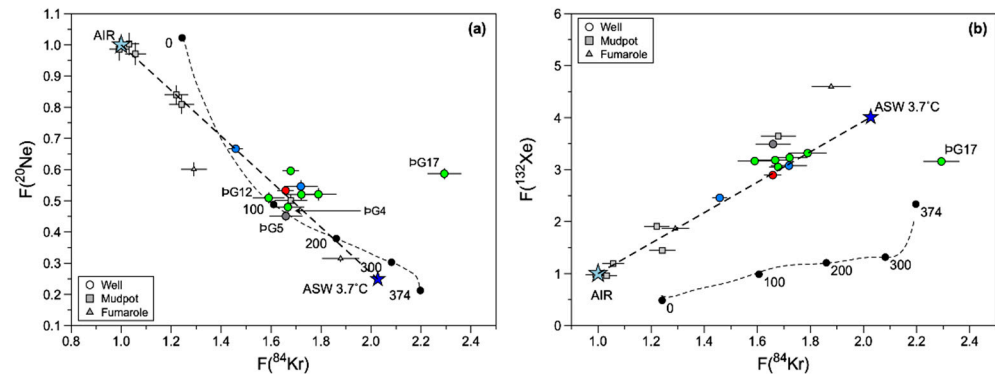


Figure 5. (a) $F(^{20}\text{Ne})$ vs. $F(^{84}\text{Kr})$, and (b) $F(^{84}\text{Kr})$ vs. $F(^{132}\text{Xe})$ measured in the surface (mudpots and fumaroles) and well fluid samples of Theistareykir. The straight lines represent the mixing between an air and an ASW component. The curves represent the solubility-controlled fractionation of $F(i)$ values in the vapor phase after fluid boiling in the reservoir (after data from [16]).

Recently, Byrne et al. [16] suggested that the variability of ANG concentrations in geothermal reservoirs, including Theistareykir, is controlled by boiling, which can fractionate the ANG ratios following their respective solubilities, as illustrated in the calculated curves reported in Figure 5a,b for the vapor phase. However, there are several lines of evidence showing that the predicted elemental fractionations proposed by [16] only partially affect the Theistareykir fluids.

Figure 6 shows that the observed variability of the ANG elemental ratios is controlled by several processes, in particular leaching Sr from basalts and mixing with ANGs and seawater via meteoric fluids. From Figure 5a,b, it is apparent that the $F(^{20}\text{Ne})$ and $F(^{84}\text{Kr})$ values (except for sample PG-17) might be either the result of mixing between meteoric water at 3.7 °C and atmospheric air, or alternatively, the mixing of a vapor phase boiled at 200 °C and atmospheric air. Air is ubiquitously present in all of the fluids of Theistareykir, both in well fluids sampled at the wellhead and surface fluids sampled at mudpots and fumaroles ([27] and Figure 5a,b). However, the $F(^{132}\text{Xe})$ value does not follow the boiling fractionation curve of Byrne et al. [16]. Instead, it seems to result from a mixture between ASW (at 3.7 °C) and the atmospheric air. If we replace $F(^{132}\text{Xe})$ with $F(^{130}\text{Xe})$ (^{132}Xe is also produced by ^{238}U fission in rocks, while ^{130}Xe is only of atmospheric origin), the trend remains unchanged, and the resulting values remain significantly different from those predicted by boiling. In order to explain this shift, Byrne et al. [16] suggested the possible addition of a sedimentary source of xenon (Xe can be adsorbed in clays and organic matter [82,83]).

The calculated $F(^{20}\text{Ne})$ values correlate with the $^{87}\text{Sr}/^{86}\text{Sr}$ ratios measured in the Theistareykir fluids (Figure 6a). The data suggest two linear trends. However, in an isotope-isotope plot, mixing leads to an hyperbola, not a straight line, unless the curvature factor “ r ” ($r = [\text{Sr}/\text{Ar}]_{\text{Basalt}}/[\text{Sr}/\text{Ar}]_{\text{Atm}}$) is 1 [84]. Here, the best fits for the two mixing hyperbolas have “ r ” values of 0.8 and 0.13, respectively (Figure 6a). In our calculations (Figure 6a), the “glacial” endmember has a seawater $^{87}\text{Sr}/^{86}\text{Sr}$ ratio of 0.709225 and atmospheric $F(^{20}\text{Ne})$ composition (i.e., $F = 1$). The second endmember has an $^{87}\text{Sr}/^{86}\text{Sr}$ ratio typical of that of the tholeiitic basalts of the Theistareykir reservoir (≤ 0.7030 [49,58]). The corresponding $F(^{20}\text{Ne})$ of the basaltic endmember is much higher than that calculated for ASW at 3.7 °C (0.249 [48]), with a value of ~ 0.42 , corresponding to an ASW component affected by boiling at 200 °C (Figure 5a).

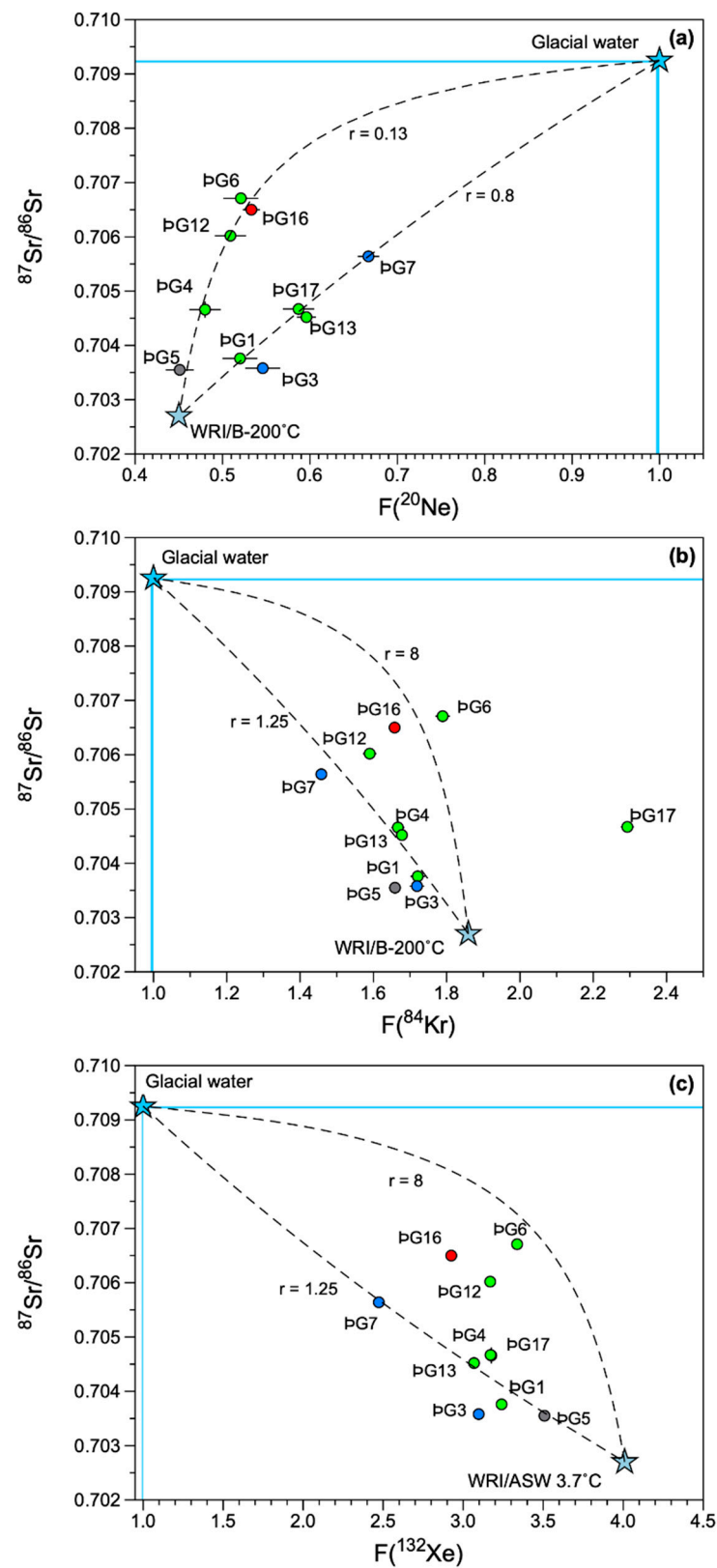


Figure 6. (a) $F(^{20}\text{Ne})$, (b) $F(^{84}\text{Kr})$ and (c) $F(^{132}\text{Xe})$ vs. $^{87}\text{Sr}/^{86}\text{Sr}$ in the well fluids of Theistareykir. The dashed lines are mixing hyperbolas between meteoric fluids leaching Sr from basalts and ANG with an ASW fractionated composition and glacial water bringing seawater Sr and ANG with an atmospheric air composition.

The $F(^{132}\text{Xe})$ and $F(^{84}\text{Kr})$ values also display a trend between the two above-defined endmembers, although it is not as clearly defined, in particular for $F(^{84}\text{Kr})$. Similarly to the $F(^{20}\text{Ne})$ findings, the $F(^{84}\text{Kr})$ value is too high (2.027 [48]) compared to that of a basaltic endmember value of ca. 1.85 (Figure 6b), and also corresponds to a fluid undergoing boiling at 200 °C (Figure 5a). However, the $F(^{132}\text{Xe})$ ASW value calculated at 3.7 °C is plausible for the basaltic endmember (Figure 6c), as is also suggested by the trend observed in Figure 5b. It is possible that the Fernández-Prini et al. [85] experimental solubility data for Xe may have been underestimated for geothermal reservoir conditions. Such a shift between the expected solubilities of xenon in geological reservoirs and what is really measured has already been observed in other situations (e.g., [86]). This underestimation would explain the observed discrepancies between Ne and Kr (Figure 6a,b) as opposed to Xe (Figure 6c).

Figure 6a,b shows two mixing hyperbolas using the same curvature factors as those obtained from the $F(^{20}\text{Ne})$ trends (the values are inverted here: $r = [\text{Sr}/\text{Ar}]_{\text{Atm}} [\text{Sr}/\text{Ar}]_{\text{Basalt}}$). The two trends encompass all of the data, except for the $F(^{84}\text{Kr})$ of sample PG17, which is more heavily impacted by a magmatic fluid endmember (Figure 3). This larger magmatic fluid impact is thought to be at the origin of the observed deviations from the expected trends for sample PG17 (Figures 5b and 6b).

5.3. ANGs and Sr: A Tracer of Glacial Meltwater Recharge

The ubiquitous presence of ANG with an atmospheric air composition in both the surface and well fluids of Theistareykir (Figures 5 and 6) could be explained by a partial recharge of the Theistareykir field by glacial water derived from snowfall. The glaciers and rainfall of Iceland contain Sr with an isotopic signature indistinguishable from seawater, which is caused by the presence of marine aerosols (the so-called “atmospheric deposition” of [53]). This is observed in the signature of non-glaciated rivers, which are replenished by these two sources of water (Figure 2). However, rainfall cannot be the source of Sr seawater in the Theistareykir geothermal fluids. Indeed, noble gas studies in rainfall (e.g., [87–89]) have highlighted the presence of different patterns for ANG other than simply atmospheric air. By contrast, ice bodies which originate from the compaction of snow (buried snowbanks, glacial ice) have ANG ratios close to those of atmospheric air because they trap air bubbles, while ice that forms from the freezing of liquid water (i.e., pingo ice) is expected to have ANG ratios similar to ASW because ANG are mainly dissolved at solubility equilibrium [90,91]. This is confirmed by the experimental data of Amalberti et al. [92], who measured the noble gas signatures in snow. This showed ANG ratios with values between those of ASW and atmospheric air, while the concentrations are strongly dependent on the snow structure. The lighter He and Ne isotopes can be accommodated in the snow crystal lattice due to their smaller atomic radii, while Ar, Kr and Xe may be hosted in inclusions of quenched water within the ice crystal because of their larger atomic radii [92].

Overall, the correlations illustrated in Figure 6a–c may result from the mixing of at least two fluids circulating in the Theistareykir geothermal reservoir. The first fluid, likely meteoric water in nature, labeled “WRI-B 200 °C”, interacts with the basaltic reservoir from which Sr is extracted from plagioclase and pyroxene. The ANGs of this fluid have elemental ratios close to ASW conditions, or slightly fractionated during boiling at 200 °C in the reservoir. The second fluid is glacial meltwater from snow or compacted-snow ice, carrying into the reservoir two unrelated sources: Sr from seawater aerosols and ANGs contained in atmospheric air bubbles trapped in the snow. The question arises whether this meteoric water component is local or distal. Most non-glaciated rivers and ice with a seawater Sr contribution (Figure 2 [52,53]) are found in S–SW Iceland. It is thus reasonable to speculate that the glacial recharge water carrying a Sr seawater component and an ANG signature in the Theistareykir is the far-south glacier recharge water from the Iceland Highlands, as suggested by [81]. The presence of large amounts of glacial water might also explain the observed differences in the Sr isotopic composition compared to the nearby Krafla and Námafjall geothermal systems. These display $^{87}\text{Sr}/^{86}\text{Sr}$ of 0.7040 ± 0.0003 [1].

These fields have water-stable isotopic compositions which are less depleted than those of Theistareykir, with values of $\delta^2\text{H} = -87\text{‰}$ and $\delta^{18}\text{O} = -12.3\text{‰}$ corresponding to the local groundwater [93].

6. Conclusions

The first Sr isotopic compositions of the Theistareykir geothermal fluids in Iceland were reported and compared with those of noble gases. In particular, the Ne/Ar ratios show a clear correlation with the $^{87}\text{Sr}/^{86}\text{Sr}$ ratios, a pattern that has not been previously observed in other geothermal areas studied using these two families of fluid tracers. Deep Theistareykir geothermal fluids have an unusual Sr isotopic and elemental composition, suggesting the presence of three sources: magmatic fluids, fluids resulting from interactions with local basaltic bedrock, and seawater. If these three sources are effectively common for all Icelandic geothermal fluids, the Sr seawater component found in Theistareykir is particularly rich. Of relevance is the observed seawater Sr signature, which appears to be related to atmospheric noble gases (ANGs). The latter display an atmospheric composition rather than an equilibrium solubility composition or ASW, as expected in meteoric water recharging geothermal reservoirs. This is thought to reflect the impact of meteoric water derived from snowpack or compacted snow ice, and may trace its recharge source to the southern glaciers of Iceland. In conclusion, we suggest that ANGs have the potential to trace meltwater recharge in geothermal fields located in glaciated areas such as Iceland.

Supplementary Materials: The following supporting information can be downloaded at <https://www.mdpi.com/article/10.3390/geosciences12030119/s1>: Table S1. Literature compilation of $^{87}\text{Sr}/^{86}\text{Sr}$ ratios measured in fluids, mineral and rocks of Iceland.

Author Contributions: Conceptualization, D.L.P., M.H.-L.; methodology, M.H.-L., A.P., M.S.; investigation, M.S.; resources, B.G., Á.K.S.; data curation, D.L.P.; writing—original draft preparation, D.L.P.; writing—review and editing, M.H.-L., M.S., V.J.v.H., K.B., A.P., M.C.C., B.G., Á.K.S.; funding acquisition, D.L.P., V.J.v.H., K.B., M.S. All authors have read and agreed to the published version of the manuscript.

Funding: This research was funded by the Natural Sciences and Engineering Research Council of Canada (NSERC) with an Alexander-Graham-Bell doctorate fellowship to M.S. (CGSD3-503679-2017), a Discovery Grant to D.L.P. (RGPIN-2015-05378), K.B. (RGPIN-2014-03882) and V.J.v.H. (RGPIN-2020-04173); a Geotop collaborative grant to D.L.P., K.B. and V.J.v.H. (no. 2018-001); NSF Instrumentation and Facilities award to M.C.C. (EAR-1049822).

Institutional Review Board Statement: Not Applicable.

Informed Consent Statement: Not Applicable.

Data Availability Statement: The data are fully reported in Table 1 in the text and Table S1 in supplemental material, except for the data of [74], which are unpublished, and are only graphically reported in Figure 3 of this study, from the homonymous publication (permission granted by Elsevier, license number 5243890193854).

Acknowledgments: We wish to thank the Landsvirkjun Iceland national power company, University of Iceland and ÍSOR for access to their facilities, and allowing sampling and logistic support.

Conflicts of Interest: The authors declare no conflict of interest.

References

1. Elderfield, H.; Greaves, M.J. Strontium isotope geochemistry of Icelandic geothermal systems and implications for sea water chemistry. *Geochim. Cosmochim. Acta* **1981**, *45*, 2201–2212. [[CrossRef](#)]
2. Notsu, K.; Wakita, H.; Nakamura, Y. Strontium isotopic composition of hot spring and mineral spring waters, Japan. *Appl. Geochem.* **1991**, *6*, 543–551. [[CrossRef](#)]
3. Graham, I.J. Strontium isotope composition of Rotorua geothermal waters. *Geothermics* **1992**, *21*, 165–180. [[CrossRef](#)]
4. Négrel, P.; Fouillac, C.; Brach, M. A strontium isotopic study of mineral and surface waters from the Cezallier (Massif Central, France): Implications for mixing processes in areas of disseminated emergences of mineral waters. *Chem. Geol.* **1997**, *135*, 89–101. [[CrossRef](#)]

5. Négrel, P.; Fouillac, C.; Brach, M. Occurrence of mineral water springs in the stream channel of the Allier River (Massif Central, France): Chemical and Sr isotope constraints. *J. Hydrol.* **1997**, *203*, 143–153. [[CrossRef](#)]
6. Négrel, P.; Guerrot, C.; Millot, R. Chemical and strontium isotope characterization of rainwater in France: Influence of sources and hydrogeochemical implications. *Isot. Environ. Health Stud.* **2007**, *43*, 179–196. [[CrossRef](#)]
7. Millot, R.; Hegan, A.; Négrel, P. Geothermal waters from the Taupo Volcanic Zone, New Zealand: Li, B and Sr isotopes characterization. *Appl. Geochem.* **2012**, *27*, 677–688. [[CrossRef](#)]
8. Mazor, E.; Truesdell, A.H. Dynamics of a geothermal field traced by noble gases: Cerro Prieto, Mexico. *Geothermics* **1984**, *13*, 91–102. [[CrossRef](#)]
9. Kennedy, B.M.; Truesdell, A.H. The Northwest Geysers high-temperature reservoir: Evidence for active magmatic degassing and implications for the origin of the Geysers geothermal field. *Geothermics* **1996**, *25*, 365–387. [[CrossRef](#)]
10. Ballentine, C.J.; Burgess, R.; Marty, B. Tracing Fluid Origin, Transport and Interaction in the Crust. *Rev. Mineral. Geochem.* **2002**, *47*, 539–614. [[CrossRef](#)]
11. Magro, G.; Ruggieri, G.; Gianelli, G.; Bellani, S.; Scandiffio, G. Helium isotopes in paleofluids and present-day fluids of the Larderello geothermal field: Constraints on the heat source. *J. Geophys. Res. Solid Earth* **2003**, *108*, ECV-3. [[CrossRef](#)]
12. Pinti, D.L.; Castro, M.C.; Shouakar-Stash, O.; Tremblay, A.; Garduño, V.H.; Hall, C.M.; Hélie, J.F.; Ghaleb, B. Evolution of the geothermal fluids at Los Azufres, Mexico, as traced by noble gas isotopes, ^{18}O , D , ^{13}C and $^{87}\text{Sr}/^{86}\text{Sr}$. *J. Volcanol. Geotherm. Res.* **2013**, *249*, 1–11. [[CrossRef](#)]
13. Roulleau, E.; Tardani, D.; Sano, Y.; Takahata, N.; Vinet, N.; Bravo, F.; Muñoz, C.; Sanchez, J. New insight from noble gas and stable isotopes of geothermal/hydrothermal fluids at Caviahue-Copahue volcanic complex: Boiling steam separation and water-rock interaction at shallow depth. *J. Volcanol. Geotherm. Res.* **2016**, *328*, 70–83. [[CrossRef](#)]
14. Norton, D.L. Theory of hydrothermal systems. *Annu. Rev. Earth Planet. Sci.* **1984**, *12*, 155–177. [[CrossRef](#)]
15. Kipfer, R.; Aeschbach-Hertig, W.; Peeters, F.; Stute, M. Noble gases in lakes and ground waters. *Rev. Mineral. Geochem.* **2002**, *47*, 615–700. [[CrossRef](#)]
16. Byrne, D.J.; Broadley, M.W.; Halldórsson, S.A.; Ranta, E.; Ricci, A.; Tyne, R.L.; Stefánsson, A.; Ballentine, C.J.; Barry, P.H. The use of noble gas isotopes to trace subsurface boiling temperatures in Icelandic geothermal systems. *Earth Planet. Sci. Lett.* **2021**, *560*, 116805. [[CrossRef](#)]
17. Allègre, C.J.; Moreira, M.; Staudacher, T. $^4\text{He}/^3\text{He}$ dispersion and mantle convection. *Geophys. Res. Lett.* **1995**, *22*, 2325–2328. [[CrossRef](#)]
18. Stuart, F.M.; Lass-Evans, S.; Fitton, J.G.; Ellam, R.M. High $^3\text{He}/^4\text{He}$ ratios in picritic basalts from Baffin Island and the role of a mixed reservoir in mantle plumes. *Nature* **2003**, *424*, 57–59. [[CrossRef](#)]
19. Broadley, M.W.; Barry, P.H.; Bekaert, D.V.; Byrne, D.J.; Caracausi, A.; Ballentine, C.J.; Marty, B. Identification of chondritic krypton and xenon in Yellowstone gases and the timing of terrestrial volatile accretion. *Proc. Nat. Acad. Sci. USA* **2020**, *117*, 13997. [[CrossRef](#)]
20. Pinti, D.L.; Castro, M.C.; López-Hernández, A.; Hernández-Hernández, M.A.; Shouakar-Stash, O.; Hall, C.M.; Bahena-Romero, J.; Ramírez-Montes, M. Origin of volatile species and aqueous fluids in the Los Humeros geothermal field, Mexico. *Chem. Geol.* **2001**, *584*, 120539. [[CrossRef](#)]
21. Pinti, D.L.; Castro, M.C.; López-Hernández, A.; Hernández-Hernández, M.A.; Richard, L.; Hall, C.M.; Shouakar-Stash, O.; Flores-Armenta, M.; Rodríguez-Rodríguez, M.H. Cerro Prieto geothermal field (Baja California, Mexico)—A fossil system? Insights from a noble gas study. *J. Volcanol. Geother. Res.* **2019**, *371*, 32–45. [[CrossRef](#)]
22. Graham, D.W. Noble Gas Isotope Geochemistry of Mid-Ocean Ridge and Ocean Island Basalts: Characterization of Mantle Source Reservoirs. *Rev. Mineral. Geochem.* **2002**, *47*, 247–317. [[CrossRef](#)]
23. Hilton, D.R.; Hammerschmidt, K.; Teufel, S.; Friedrichsen, H. Helium isotope characteristics of Andean geothermal fluids and lavas. *Earth Planet. Sci. Lett.* **1993**, *120*, 265–282. [[CrossRef](#)]
24. Poreda, R.; Craig, H. Helium isotope ratios in circum-pacific volcanic arcs. *Nature* **1989**, *338*, 473–478. [[CrossRef](#)]
25. van Soest, M.C.; Hilton, D.R.; Kreulen, R. Tracing crustal and slab contributions to arc magmatism in the Lesser Antilles Island arc using helium and carbon relationships in geothermal fluids. *Geochim. Cosmochim. Acta* **1998**, *62*, 3323–3335. [[CrossRef](#)]
26. Wen, T.; Pinti, D.L.; Castro, M.C.; López-Hernández, A.; Hall, C.M.; Shouakar-Stash, O.; Sandoval-Medina, F. A noble gas and $^{87}\text{Sr}/^{86}\text{Sr}$ study in fluids of the Los Azufres geothermal field, Mexico—Assessing impact of exploitation and constraining heat sources. *Chem. Geol.* **2018**, *483*, 426–441. [[CrossRef](#)]
27. Saby, M.; Pinti, D.L.; van Hinsberg, V.; Gautason, B.; Sigurðardóttir, Á.; Castro, M.C.; Hall, C.M.; Óskarsson, F.; Rocher, O.; Hélie, J.-F.; et al. Sources and transport of fluid and heat at the newly-developed Theistareykir geothermal field, Iceland. *J. Volcanol. Geother. Res.* **2020**, *405*, 107062. [[CrossRef](#)]
28. Kennedy, B.M.; Shuster, D.L. Noble gases: Sensitive natural tracers for detection and monitoring injectate returns to geothermal reservoirs. *GRC Trans.* **2000**, *24*, 247–252.
29. Khodayar, M.; Björnsson, S.; Kristinsson, S.G.; Karlsdóttir, R.; Ólafsson, M.; Víkingsson, S. Tectonic control of the Theistareykir geothermal field by rift and transform zones in North Iceland: A multidisciplinary approach. *Open J. Geol.* **2018**, *8*, 543–584. [[CrossRef](#)]

30. Þorsteinsdóttir, U.; Guðmundsdóttir, V.; Árnadóttir, S.; Blischke, A.; Gautason, B.; Mortensen, A. The Þeistareykir geothermal field, NE Iceland: Sub-surface structural analysis based on borehole televiwer imaging. In Proceedings of the World Geothermal Congress 2020+1, Reykjavik, Iceland, 24–27 October 2021.
31. Ármannsson, H.; Gíslason, G.; Torfason, H. Surface exploration of the Þeistareykir high-temperature geothermal area, Iceland, with special reference to the application of geochemical methods. *Appl. Geochem.* **1986**, *1*, 47–64. [[CrossRef](#)]
32. MacLennan, J.; Jull, M.; McKenzie, D.; Slater, L.; Grönvold, K. The link between volcanism and deglaciation in Iceland. *Geochem. Geophys. Geosyst.* **2002**, *3*, 1–25. [[CrossRef](#)]
33. Sæmundsson, K. The Geology of Þeistareykir (in Icelandic). In *Iceland GeoSurvey, Short Report ÍSOR-07270 (in Icelandic)*; ISOR: Reykjavik, Iceland, 2007; p. 23.
34. Yu, G.; Gunnarsson, Á.; He, Z.; Tulinius, H. Characterizing a geothermal reservoir using broadband 2-D MT survey in Þeistareykir, Iceland. In Proceedings of the World Geothermal Congress 2010, Bali, Indonesia, 25–29 April 2010.
35. Kajugus, S.I. *Updated Reservoir Analysis of the Þeistareykir High-Temperature Geothermal Field, N-Iceland*; Report 15; Geothermal Training Programme, United Nations University: Reykjavik, Iceland, 2012; p. 28.
36. Guðfinnsson, G.H. *Alteration in the Þeistareykir Geothermal System. A Study of Drill Cuttings in Thin Sections*; Report LV-2014-063; Landsvirkjun: Reykjavik, Iceland, 2014; p. 107.
37. Óskarsson, F. Exploration and development of a conceptual model for the Þeistareykir geothermal field, NE-Iceland. In Proceedings of the Short Course VII on Exploration for Geothermal Resources, Lake Bogoria and Lake Naivasha, Kenya, 9–19 November 2017.
38. Mutch, E.J.F.; MacLennan, J.; Shorttle, O.; Edmonds, M.; Rudge, J.F. Rapid transcrustal magma movement under Iceland. *Nature Geosci.* **2019**, *12*, 569–574. [[CrossRef](#)]
39. Óskarsson, F.; Ármannsson, H.; Ólafsson, M.; Sveinbjörnsdóttir, Á.E.; Markússon, S.H. The Þeistareykir geothermal field, NE Iceland: Fluid chemistry and production properties. *Proc. Earth Planet. Sci.* **2013**, *7*, 644–647. [[CrossRef](#)]
40. Stefánsson, A.; Hilton, D.R.; Sveinbjörnsdóttir, Á.E.; Torssander, P.; Heinemeier, J.; Barnes, J.D.; Ono, S.; Halldórsson, S.A.; Fiebig, J.; Arnórsson, S. Isotope systematics of Icelandic thermal fluids. *J. Volcano. Geother. Res.* **2017**, *337*, 146–164. [[CrossRef](#)]
41. Darling, W.G.; Ármannsson, H. stable isotopic aspects of fluid flow in the Krafla, Námafjall and Þeistareykir geothermal systems of Northeast Iceland. *Chem. Geol.* **1989**, *76*, 197–213. [[CrossRef](#)]
42. Hauksson, T. *Þeistareykir, Krafla Og Bjarnarflag. Afköst Borhola Og Efnainnihald Vatns Og Gufu Í Borholum Og Vinnslurás Árið 2019*; Report LV-2020-010; Landsvirkjun: Reykjavik, Iceland, 2020; p. 77.
43. Tardani, D.; Roulleau, E.; Pinti, D.L.; Pérez-Flores, P.; Daniele, L.; Reich, M.; Sanchez-Alfaro, P.; Morata, D.; Richard, L. Structural control on shallow hydrogeochemical processes at Caviahue-Copahue Volcanic Complex (CCVC), Argentina. *J. Volcanol. Geother. Res.* **2021**, *414*, 107228. [[CrossRef](#)]
44. Hiyagon, H.; Kennedy, B.M. Noble gases in CH₄-rich gas fields, Alberta, Canada. *Geochim. Cosmochim. Acta* **1992**, *56*, 1569–1589. [[CrossRef](#)]
45. Kuhn, T.; Herzig, P.M.; Hannington, M.D.; Garbe-Schönberg, D.; Stoffers, P. Origin of fluids and anhydrite precipitation in the sediment-hosted Grimsey hydrothermal field North of Iceland. *Chem. Geol.* **2003**, *202*, 5–21. [[CrossRef](#)]
46. Edmond, J.M.; Measures, C.; McDuff, R.E.; Chan, L.H.; Collier, R.; Grant, B.; Gordon, L.I.; Corliss, J.B. Ridge crest hydrothermal activity and the balances of the major and minor elements in the ocean: The Galapagos data. *Earth Planet. Sci. Lett.* **1979**, *46*, 1–18. [[CrossRef](#)]
47. Smith, S.P.; Kennedy, B.M. The solubility of noble gases in water and NaCl brine. *Geochim. Cosmochim. Acta* **1983**, *47*, 503–515. [[CrossRef](#)]
48. Benson, B.B.; Krause, D., Jr. Empirical laws for dilute aqueous solutions of non-polar gases. *J. Chem. Phys.* **1976**, *64*, 689–709. [[CrossRef](#)]
49. Stracke, A.; Zindler, A.; Salters, V.J.M.; McKenzie, D.; Blichert-Toft, J.; Albarède, F.; Grönvold, K. Þeistareykir revisited. *Geochem. Geophys. Geosyst.* **2003**, *4*, 1–49. [[CrossRef](#)]
50. Fox, S.; Katzir, Y.; Bach, W.; Schlicht, L.; Glessner, J. Magmatic volatiles episodically flush oceanic hydrothermal systems as recorded by zoned epidote. *Commun. Earth Environ.* **2020**, *1*, 52. [[CrossRef](#)]
51. Marks, N.; Zierenberg, R.A.; Schiffman, P. Strontium and oxygen isotopic profiles through 3 km of hydrothermally altered oceanic crust in the Reykjanes geothermal system, Iceland. *Chem. Geol.* **2015**, *412*, 34–47. [[CrossRef](#)]
52. Hindshaw, R.S.; Bourdon, B.; Pogge von Strandmann, P.A.E.; Vigier, N.; Burton, K.V. The stable calcium isotopic composition of rivers draining basaltic catchments in Iceland. *Earth Planet. Sci. Lett.* **2013**, *374*, 173–184. [[CrossRef](#)]
53. Andrews, M.G.; Jacobson, A.D. The radiogenic and stable sr isotope geochemistry of basalt weathering in Iceland: Role of hydrothermal calcite and implications for long-term climate regulation. *Geochim. Cosmochim. Acta* **2017**, *215*, 247–262. [[CrossRef](#)]
54. Óskarsson, F. The origin of the warm groundwater near Lake Mývatn, NE Iceland, traced by stable isotopes. In *E3S Web of Conferences*; EDP Sciences: Ulis, France, 2019; Volume 98, p. 5.
55. Fowler, A.P.G.; Zierenberg, R.A.; Schiffman, P.; Marks, N.; Friðleifsson, G.Ó. Evolution of fluid–rock interaction in the Reykjanes geothermal system, Iceland: Evidence from Iceland Deep Drilling Project Core Rn-17b. *J. Volcanol. Geother. Res.* **2015**, *302*, 47–63. [[CrossRef](#)]
56. O’Nions, R.K.; Grönvold, K. Petrogenetic relationships of acid and basic rocks in Iceland: Sr-Isotopes and Rare-Earth Elements in late and postglacial volcanics. *Earth Planet. Sci. Lett.* **1973**, *19*, 397–409. [[CrossRef](#)]

57. O’Nions, R.K.; Pankhurst, R.J. Secular variation in the Sr-isotope composition of Icelandic volcanic rocks. *Earth Planet. Sci. Lett.* **1973**, *21*, 13–21. [[CrossRef](#)]
58. O’Nions, R.K.; Pankhurst, R.J.; Grönvold, K. Nature and development of basalt magma sources beneath Iceland and the Reykjanes Ridge. *J. Petrol.* **1976**, *17*, 315–338. [[CrossRef](#)]
59. Zindler, A.; Hart, S.R.; Frey, F.A.; Jakobsson, S.P. Nd and Sr isotope ratios and rare earth element abundances in Reykjanes Peninsula basalts evidence for mantle heterogeneity beneath Iceland. *Earth Planet. Sci. Lett.* **1979**, *45*, 249–262. [[CrossRef](#)]
60. Condomines, M.; Grönvold, K.; Hooker, P.J.; Muehlenbachs, K.; O’Nions, R.K.; Óskarsson, N.; Oxburgh, E.R. Helium, oxygen, strontium and neodymium isotopic relationships in Icelandic volcanics. *Earth Planet. Sci. Lett.* **1983**, *66*, 125–136. [[CrossRef](#)]
61. Furman, T.; Frey, F.A.; Park, K.-H. Chemical constraints on the petrogenesis of mildly alkaline lavas from Vestmannaeyjar, Iceland: The Eldfell (1973) and Surtsey (1963–1967) eruptions. *Contrib. Mineral. Petrol.* **1991**, *109*, 19–37. [[CrossRef](#)]
62. Nicholson, H.; Condomines, M.; Godfrey Fitton, J.; Fallick, A.E.; Grönvold, K.; Rogers, G. Geochemical and isotopic evidence for crustal assimilation beneath Krafla, Iceland. *J. Petrol.* **1991**, *32*, 1005–1020. [[CrossRef](#)]
63. Sigmarsson, O.; Condomines, M.; Fourcade, S. Mantle and crustal contribution in the genesis of recent basalts from off-rift zones in Iceland: Constraints from Th, Sr and O isotopes. *Earth Planet. Sci. Lett.* **1992**, *110*, 149–162. [[CrossRef](#)]
64. Hemond, C.; Arndt, N.T.; Lichtenstein, U.; Hofmann, A.W.; Óskarsson, N.; Steinthorsson, S. The heterogeneous Iceland plume: Nd-Sr-O isotopes and trace element constraints. *J. Geophys. Res. Solid Earth* **1993**, *98*, 15833–15850. [[CrossRef](#)]
65. Gee, M.A.M.; Thirlwall, M.F.; Taylor, R.N.; Lowry, D.; Murton, B.J. Crustal processes: Major controls on Reykjanes Peninsula lava chemistry, SW Iceland. *J. Petrol.* **1998**, *39*, 819–839. [[CrossRef](#)]
66. Breddam, K. Kistufell: Primitive melt from the Iceland mantle plume. *J. Petrol.* **2002**, *43*, 345–373. [[CrossRef](#)]
67. Kokfelt, T.F.; Hoernle, K.A.J.; Hauff, F.; Fiebig, J.; Werner, R.; Garbe-Schönberg, D. Combined trace element and Pb-Nd-Sr-O isotope evidence for recycled oceanic crust (Upper and Lower) in the Iceland mantle plume. *J. Petrol.* **2006**, *47*, 1705–1749. [[CrossRef](#)]
68. Lacasse, C.; Sigurdsson, H.; Carey, S.N.; Jóhannesson, H.; Thomas, L.E.; Rogers, N.W. Bimodal volcanism at the Katla subglacial caldera, Iceland: Insight into the geochemistry and petrogenesis of rhyolitic magmas. *Bull. Volcanol.* **2006**, *69*, 373–399. [[CrossRef](#)]
69. Martin, E.; Sigmarsson, O. Thirteen million years of silicic magma production in Iceland: Links between petrogenesis and tectonic settings. *Lithos* **2010**, *116*, 129–144. [[CrossRef](#)]
70. Peate, D.W.; Breddam, K.; Baker, J.A.; Kurz, M.D.; Barker, A.K.; Prestvik, T.; Grassineau, N.; Skovgaard, A.C. Compositional characteristics and spatial distribution of enriched Icelandic mantle components. *J. Petrol.* **2010**, *51*, 1447–1475. [[CrossRef](#)]
71. Shorttle, O.; MacLennan, J.; Piotrowski, A.M. Geochemical provincialism in the Iceland plume. *Geochim. Cosmochim. Acta* **2013**, *122*, 363–397. [[CrossRef](#)]
72. Zierenberg, R.A.; Schiffman, P.; Barfod, G.H.; Leshner, C.E.; Marks, N.E.; Lowenstern, J.B.; Mortensen, A.K.; Pope, E.C.; Bird, D.K.; Reed, M.H.; et al. Composition and origin of rhyolite melt intersected by drilling in the Krafla geothermal field, Iceland. *Contrib. Mineral. Petrol.* **2013**, *165*, 327–347. [[CrossRef](#)]
73. Sigmarsson, O.; Halldórsson, S.A. Delimiting Baroarbunga and Askja volcanic systems with Sr- and Nd-isotope ratios. *Jökull* **2015**, *65*, 17–28.
74. Millot, R.; Ásmundsson, R.; Négrel, P.; Sanjuan, B.; Bullen, T. Multi-isotopic (H, O, C, S, Li, B, Si, Sr, Nd) approach for geothermal fluid characterization in Iceland. *Geochim. Cosmochim. Acta* **2009**, *73*, A883, abstract.
75. Kelemen, P.B.; Hanghøj, K.; Greene, A.R. 3.18—One View of the Geochemistry of Subduction-Related Magmatic Arcs, with an Emphasis on Primitive Andesite and Lower Crust. In *Treatise on Geochemistry*, 2nd ed.; Holland, H.D., Turekian, K.K., Eds.; Pergamon: Oxford, UK, 2007; Volume 3, pp. 1–70.
76. Arnórsson, S.; Andrésdóttir, A. Processes controlling the distribution of boron and chlorine in natural waters in Iceland. *Geochim. Cosmochim. Acta* **1995**, *59*, 4125–4146. [[CrossRef](#)]
77. Clark, I.D. *Groundwater Geochemistry and Isotopes*, 1st ed.; CRC Press: Boca Raton, FL, USA, 2015; p. 442.
78. Eiríksdóttir, E.S.; Sigurdsson, Á.; Gíslason, S.R.; Torssander, P. Chemical composition of precipitation and river water in Southern Iceland: Effects of Eyjafjallajökull volcanic eruptions and geothermal power plants. *Proc. Earth Planet. Sci.* **2014**, *10*, 358–364. [[CrossRef](#)]
79. Bragason, G.Ö. Strontium Isotope Shift in Clay Minerals, Epidote and Geothermal Fluid in the Hellisheiði Geothermal Field, SW-Iceland. Master’s Thesis, University of Iceland, Reykjavik, Iceland, 2012.
80. Junge, C.E.; Werby, R.T. The Concentration of Chloride, Sodium, Potassium, Calcium, and Sulfate in rain water over the United States. *J. Atm. Sci.* **1958**, *15*, 417–425. [[CrossRef](#)]
81. Sveinbjörnsdóttir, Á.E.; Ármannsson, H.; Ólafsson, M.; Óskarsson, F.; Markússon, S.; Magnúsdóttir, S. The Theistareykir Geothermal Field, NE Iceland. Isotopic characteristics and origin of circulating fluids. *Proc. Earth Planet. Sci.* **2013**, *7*, 822–825. [[CrossRef](#)]
82. Bernatowicz, T.J.; Podosek, F.A.; Honda, M.; Kramer, F.E. The atmospheric inventory of xenon and noble gases in shales: The plastic bag experiment. *J. Geophys. Res. Solid Earth* **1984**, *89*, 4597–4611. [[CrossRef](#)]
83. Pitre, F.; Pinti, D.L. Noble gas enrichments in porewater of estuarine sediments and their effect on the estimation of net denitrification rates. *Geochim. Cosmochim. Acta* **2010**, *74*, 531–539. [[CrossRef](#)]
84. Langmuir, C.H.; Vocke, R.D.; Hanson, G.N.; Hart, S.R. A general mixing equation with applications to Icelandic basalts. *Earth Planet. Sci. Lett.* **1978**, *37*, 380–392. [[CrossRef](#)]

85. Fernández-Prini, R.; Alvarez, J.L.; Harvey, A.H. Henry's constants and vapor–liquid distribution constants for gaseous solutes in H₂O and D₂O at high temperatures. *J. Phys. Chem. Ref. Data* **2003**, *32*, 903–916. [[CrossRef](#)]
86. Ballentine, C.J.; O'Nions, R.K.; Coleman, M.L. A Magnus Opus: Helium, neon, and argon isotopes in a North Sea oilfield. *Geochim. Cosmochim. Acta* **1996**, *60*, 831–849. [[CrossRef](#)]
87. Warrier, R.B.; Castro, M.C.; Hall, C.M.; Lohmann, K.C. Noble gas composition in rainwater and associated weather patterns. *Geophys. Res. Lett.* **2013**, *40*, 3248–3252. [[CrossRef](#)]
88. Niu, Y.; Castro, M.C.; Hall, C.M.; Gingerich, S.B.; Scholl, M.A.; Warrier, R.B. Noble gas signatures in the Island of Maui, Hawaii: Characterizing groundwater sources in fractured systems. *Water Resour. Res.* **2017**, *53*, 3599–3614. [[CrossRef](#)]
89. Hall, C.M.; Castro, M.C.; Scholl, M.A.; Amalberti, J.; Gingerich, S.B. Anomalous noble gas solubility in liquid cloud water: Possible implications for noble gas temperatures and cloud physics. *Water Resour. Res.* **2021**, *57*, e2020WR029306. [[CrossRef](#)]
90. Utting, N.; Lauriol, B.; Lacelle, D.; Clark, I.D. Using noble gas ratios to determine the origin of ground ice. *Quarter. Res.* **2016**, *85*, 177–184. [[CrossRef](#)]
91. Malone, J.L.; Castro, M.C.; Hall, C.M.; Doran, P.T.; Kenig, F.; McKay, C.P. New insights into the origin and evolution of Lake Vida, McMurdo Dry Valleys, Antarctica—A noble gas study in ice and brines. *Earth Planet. Sci. Lett.* **2010**, *289*, 112–122. [[CrossRef](#)]
92. Amalberti, J.; Hall, C.M.; Castro, M.C. Noble Gas Signatures in Snow. *Chem. Geol.* **2018**, *483*, 275–285. [[CrossRef](#)]
93. Pope, E.C.; Bird, D.K.; Arnórsson, S.; Giroud, N. Hydrogeology of the Krafla geothermal system, Northeast Iceland. *Geofluids* **2016**, *16*, 175–197. [[CrossRef](#)]